THE FOCUSED FIELDS OF FRESNEL ZONE PLATE LENS*

Guo Zhong JIANG Wen Xun ZHANG Kai KANG
State Key Lab. of Millimeter Waves, Southeast University
Nanjing 210096 CHINA

INTRODUCTION

Because of its low cost, light weight, and easy fabrication , the Fresnel Zone Plate (FZP) Antenna is becoming an important candidate for such applications as DBS reception and mobile communication. Since the fact of feed blockage in FZP reflector [1], the study of FZP lens is excited. In this paper a dual-layer FZP lens (Fig.1) is proposed to enhance the aperture efficiency, the field intensity in focal region under plane wave normal incidence is studied, and compared with single-layer FZP lens. An improved full-wave analysis based on vector Hankel transform and spectral domain immitance matrix approach is developed, with several attractive features: 1) the Green's functions in spectral domain can be derived by using equivalent transmission line method; 2) only single integration are required; 3) only low-order matrix is to be dealt with. Numerical results match the physical characteristics of FZP lens.

ANALYSIS

The transverse components of electromagnetic fields ($E_\rho, E_\varphi, H_\rho, H_\varphi$) in FZP structure (Fig.1) holding hybrid modes ($TM^z + TE^z$) can be formulated by both electric and magnetic Hertz potentials π^e and π^h in $\hat{z}$ direction with time-harmonic factor $e^{j\omega t}$ and periodic factor $e^{jn\varphi}$ (both are omitted below) as follows:

$$\mathbf{E}_{\perp n} = \begin{bmatrix} E_{\rho n}(\rho,z) \\ E_{\varphi n}(\rho,z) \end{bmatrix} = \begin{bmatrix} \frac{\partial}{\partial\rho}\frac{\partial}{\partial z} & \omega\mu\frac{n}{\rho} \\ \frac{jn}{\rho}\frac{\partial}{\partial z} & j\omega\mu\frac{\partial}{\partial\rho} \end{bmatrix} \begin{bmatrix} \pi_n^e(\rho,z) \\ \pi_n^h(\rho,z) \end{bmatrix}, \quad \mathbf{H}_{\perp n} = \begin{bmatrix} H_{\rho n}(\rho,z) \\ H_{\varphi n}(\rho,z) \end{bmatrix} = \begin{bmatrix} \frac{\partial}{\partial\rho}\frac{\partial}{\partial z} & -\omega\varepsilon\frac{n}{\rho} \\ \frac{jn}{\rho}\frac{\partial}{\partial z} & -j\omega\varepsilon\frac{\partial}{\partial\rho} \end{bmatrix} \begin{bmatrix} \pi_n^h(\rho,z) \\ \pi_n^e(\rho,z) \end{bmatrix} \quad (1)$$

Introducing the vector Hankel transform pair [3]:

$$\tilde{\mathbf{f}}_n(k_\rho) = \int_0^\infty \mathcal{H}_n(k_\rho\rho)\,\mathbf{f}_n(\rho)\rho d\rho, \qquad \mathbf{f}_n(\rho) = \int_0^\infty \mathcal{H}_n(k_\rho\rho)\,\tilde{\mathbf{f}}_n(k_\rho)k_\rho dk_\rho \quad (2)$$

where $\tilde{\mathbf{f}}_n(k_\rho) = \begin{bmatrix} \tilde{f}_{1n}(k_\rho) \\ \tilde{f}_{2n}(k_\rho) \end{bmatrix}$, $\mathbf{f}_n(\rho) = \begin{bmatrix} f_{1n}(\rho) \\ f_{2n}(\rho) \end{bmatrix}$, $\mathcal{H}_n(k_\rho\rho) = \begin{bmatrix} J_n'(k_\rho\rho) & -j\frac{n}{k_\rho\rho}J_n(k_\rho\rho) \\ j\frac{n}{k_\rho\rho}J_n(k_\rho\rho) & J_n'(k_\rho\rho) \end{bmatrix}$

$J_n(\bullet)$ and $J_n'(\bullet)$ are the Bessel function and its derivative, respectively,

the fields $\tilde{\mathbf{E}}_{\perp n}$ and $\tilde{\mathbf{H}}_{\perp n}$ in spectral domain may be expressed as:

$$\tilde{\mathbf{E}}_{\perp n} = \begin{bmatrix} \tilde{E}_{\rho n} \\ \tilde{E}_{\varphi n} \end{bmatrix} = \int_0^\infty \rho d\rho \begin{bmatrix} \mathcal{L}_1 & 0 \\ 0 & \mathcal{L}_2 \end{bmatrix} \begin{bmatrix} \pi^e \\ \pi^h \end{bmatrix}, \quad \tilde{\mathbf{H}}_{\perp n} = \begin{bmatrix} \tilde{H}_{\rho n} \\ \tilde{H}_{\varphi n} \end{bmatrix} = \int_0^\infty \rho d\rho \begin{bmatrix} 0 & \mathcal{L}_3 \\ \mathcal{L}_4 & 0 \end{bmatrix} \begin{bmatrix} \pi^e \\ \pi^h \end{bmatrix} \quad (3)$$

*This work is supported by the National Natural Science Fund (No.69571009) of China

with the operators:

$$\mathcal{L}_1=\mathcal{L}_3=\left[J_n'(k_\rho\rho)\frac{\partial}{\partial\rho}+\frac{n^2}{k_\rho\rho^2}J_n(k_\rho\rho)\right]\frac{\partial}{\partial z}\ ,\quad \mathcal{L}_2=-\frac{\varepsilon}{\mu}\mathcal{L}_4=j\omega\mu\left[J_n'(k_\rho\rho)\frac{\partial}{\partial\rho}+\frac{n^2}{k_\rho\rho^2}J_n(k_\rho\rho)\right]$$

Thus the hybrid modes in spatial domain are decomposed into independent *TM* modes ($\tilde{E}_{zn},\tilde{E}_{\rho n},\tilde{H}_{\varphi n}$) due to π^e and *TE* modes ($\tilde{H}_{zn},\tilde{E}_{\varphi n},\tilde{H}_{\rho n}$) due to π^h in spectral domain. Furthermore, the vector Hankel transform of the magnetic-field boundary condition on the patches from spatial to spectral domain are:

$$\begin{bmatrix}\tilde{H}_{\rho n1}\\ \tilde{H}_{\varphi n1}\end{bmatrix}-\begin{bmatrix}\tilde{H}_{\rho n2}\\ \tilde{H}_{\varphi n2}\end{bmatrix}=\begin{bmatrix}\tilde{I}_{\rho n}\\ \tilde{I}_{\varphi n}\end{bmatrix}=\int_0^\infty \mathcal{H}(k_\rho\rho)\begin{bmatrix}I_{\rho n}\\ I_{\varphi n}\end{bmatrix}\rho d\rho \tag{4}$$

where $\tilde{I}_{\rho n}$ and $\tilde{I}_{\varphi n}$ correspond to the *TM* and *TE* modes, respectively.

By means of the viewpoint of equivalent transmission lines (Fig.2), the propagation constant is $\gamma^2=k_\rho^2-k_0^2$, the wave admittances are $Y_c^e=j\omega\varepsilon_0/\gamma$, $Y_c^h=\gamma/j\omega\mu_0$. The Green's function, i.e. the electric fields produced by unit current source may be understood as impedance elements in the matrix equation:

$$\begin{bmatrix}\tilde{\mathbf{E}}_{\perp n1}\\ \tilde{\mathbf{E}}_{\perp n2}\end{bmatrix}=\begin{bmatrix}[\tilde{z}_{11}] & [\tilde{z}_{12}]\\ [\tilde{z}_{21}] & [\tilde{z}_{22}]\end{bmatrix}\begin{bmatrix}\tilde{\mathbf{I}}_{n1}\\ \tilde{\mathbf{I}}_{n2}\end{bmatrix} \tag{5}$$

where $\left[\tilde{\mathbf{E}}_{\perp ni}\right]=\begin{bmatrix}\tilde{E}_{\rho ni}\\ \tilde{E}_{\varphi ni}\end{bmatrix}$, $\left[\tilde{\mathbf{I}}_{\perp ni}\right]=\begin{bmatrix}\tilde{I}_{\rho ni}\\ \tilde{I}_{\varphi ni}\end{bmatrix}$, $\left[\tilde{z}_{ij}\right]=\begin{bmatrix}\tilde{z}_{ij}^{\,e} & 0\\ 0 & \tilde{z}_{ij}^{\,h}\end{bmatrix}$, $\tilde{z}_{ij}^{e,h}=e^{-\gamma|z_j-z_i|}/2Y_c^{e,h}$ $(i,j=1,2)$.

Substitute (5) into electric-field boundary condition on the patches, a couple of integral equations of $\tilde{\mathbf{I}}_{ni}$ is modelled as :

$$\begin{bmatrix}E_{\rho ni}\\ E_{\varphi ni}\end{bmatrix}=\int_0^\infty \mathcal{H}_n(k_\rho\rho)\begin{bmatrix}[z_{11}] & [z_{12}]\\ [z_{21}] & [z_{22}]\end{bmatrix}\begin{bmatrix}\tilde{I}_{\rho ni}\\ \tilde{I}_{\varphi ni}\end{bmatrix}k_\rho dk_\rho=-\begin{bmatrix}E_{\rho ni}^{inc}\\ E_{\varphi ni}^{inc}\end{bmatrix} \tag{6}$$

By the Galerkin's procedure, the spectral current in (6) is expanded as:

$$\tilde{\mathbf{I}}_{ni}=\begin{bmatrix}\tilde{I}_{\rho ni}\\ \tilde{I}_{\varphi ni}\end{bmatrix}=\sum_{l=1}^{L}\left(\sum_{m=1}^{M}\alpha_{nilm}\tilde{\mathbf{e}}_{nilm}+\sum_{p=1}^{P}\beta_{nilp}\tilde{\mathbf{h}}_{nilp}\right) \tag{7}$$

where the basis functions $\{\tilde{\mathbf{e}}_{nilm},\tilde{\mathbf{h}}_{nilp}\}$ transformed from the eigen-functions $\{\mathbf{e}_{nilm},\mathbf{h}_{nilp}\}$ defined on the rings bounded by $r_{il+}=\sqrt{2l\lambda F_i/v+(l\lambda/v)^2}$ and $r_{il-}=\sqrt{(2l-1)\lambda F_i/v+(2l-1/2v)^2}$ in spatial domain for *TM* and *TE* modes[2] respectively, where $i=1,2$ means the number of layer; $l=1,2,\cdots$ means the number of Fresnel ring in each plate, and F_i is the i-th focal of FZP.

$$\tilde{\mathbf{e}}_{nilm}=\begin{bmatrix}\dfrac{-x'_{nilm}}{k_\rho^2-x'^2_{nilm}}\left(r_{il+}J_n'(k_\rho r_{il+})\psi^e_{nilm}(r_{il+})-r_{il-}J_n'(k_\rho r_{il-})\psi^e_{nilm}(r_{il-})\right)\\ j\dfrac{n}{k_\rho x'_{nilm}}\left(J_n(k_\rho r_{il+})\psi^e_{nilm}(r_{il+})-J_n(k_\rho r_{il-})\psi^e_{nilm}(r_{il-})\right)\end{bmatrix},$$

$$\tilde{\mathbf{h}}_{nilp}=\begin{bmatrix}0\\ j\dfrac{k_\rho}{k_\rho^2-x^2_{nilp}}\left(r_{il+}J_n(k_\rho r_{il+})\psi^{h'}_{nilp}(r_{il+})-r_{il-}J_n(k_\rho r_{il-})\psi^{h'}_{nilm}(r_{il-})\right)\end{bmatrix} \tag{8}$$

where

$$\psi^{e}_{nilm}(\rho) = N'_n(x'_{nilm} r_{il-})J_n(x'_{nilm}\rho) - J'_n(x'_{nilm} r_{il-})N_n(x'_{nilm}\rho)$$

$$\psi^{h}_{nilp}(\rho) = N_n(x_{nimp} r_{il-})J_n(x_{nilp}\rho) - J_n(x_{nilp} r_{il-})N_n(x_{nilp}\rho)$$

x'_{nilm} is the m-th root of $\psi^{e'}_{nilm}$, x_{nilp} is the p-th root of $\psi^{h'}_{nilp}$, the Hermitain inner-products with $\{\rho\tilde{\mathbf{e}}_{nilm}, \rho\tilde{\mathbf{h}}_{nilp}\}$ are taken for equation (6), also the Parseval's theorem for vector Hankel transform should be employed. Finally a set of simultaneous algebraic equations is formulated in the matrix form as:

$$\begin{bmatrix} [A^{ee}_{11}] & [A^{ee}_{12}] & [A^{eh}_{11}] & [A^{eh}_{12}] \\ [A^{ee}_{21}] & [A^{ee}_{22}] & [A^{eh}_{21}] & [A^{eh}_{22}] \\ [A^{he}_{11}] & [A^{he}_{12}] & [A^{hh}_{11}] & [A^{hh}_{12}] \\ [A^{he}_{21}] & [A^{he}_{22}] & [A^{hh}_{21}] & [A^{hh}_{22}] \end{bmatrix} \begin{bmatrix} [\alpha_1] \\ [\alpha_2] \\ [\beta_1] \\ [\beta_2] \end{bmatrix} = \begin{bmatrix} [F^e_1] \\ [F^e_2] \\ [F^h_1] \\ [F^h_2] \end{bmatrix} \tag{9}$$

where: $A^{ee}_{ij} = \int_0^\infty k_\rho dk_\rho \tilde{\mathbf{e}}^*_{nir'ni}[\tilde{z}_{ij}]\tilde{\mathbf{e}}_{njlm}$, $A^{eh}_{ij} = \int_0^\infty k_\rho dk_\rho \tilde{\mathbf{e}}^*_{nir'ni}[\tilde{z}_{ij}]\tilde{\mathbf{h}}_{njlp}$, $F^e_i = \int_{r_{ir-}}^{r_{ir+}} (\mathbf{e}^*_{nir'ni} \cdot \mathbf{E}^{inc}_n)\rho d\rho$

$A^{he}_{ij} = \int_0^\infty k_\rho dk_\rho \tilde{\mathbf{h}}^*_{nir'p'}[\tilde{z}_{ij}]\tilde{\mathbf{e}}_{njlm}$, $A^{hh}_{ij} = \int_0^\infty k_\rho dk_\rho \tilde{\mathbf{h}}^*_{nir'p'}[\tilde{z}_{ij}]\tilde{\mathbf{h}}_{njlp}$, $F^h_i = \int_{r_{ir-}}^{r_{ir+}} (\mathbf{h}^*_{nir'p'} \cdot \mathbf{E}^{inc}_n)\rho d\rho$

The current expansion coefficients (α_i, β_i) can be solved from (9). By using equivalent transmission lines (Fig.2), we get the spectral scattered electric field components in the focal region of a dual-layer FZP lens as follows:

$$\begin{bmatrix} \tilde{E}^{sc}_{\rho n} \\ \tilde{E}^{sc}_{\varphi n} \end{bmatrix} = \sum_{k=1}^{2}\sum_{l=1}^{L} \begin{bmatrix} \tilde{E}^{sc}_{\rho nilm}(z) \\ \tilde{E}^{sc}_{\varphi nilm}(z) \end{bmatrix}, \begin{bmatrix} \tilde{E}^{sc}_{\rho nilm}(z) \\ \tilde{E}^{sc}_{\varphi nilm}(z) \end{bmatrix} = \frac{e^{-\gamma|z-z_i|}}{2} \begin{bmatrix} 1/Y^e_c & 0 \\ 0 & 1/Y^h_c \end{bmatrix} \begin{bmatrix} \tilde{J}_{\rho i} \\ \tilde{J}_{\varphi i} \end{bmatrix} \tag{10}$$

Since hybrid modes in spectral domain have been decomposed into independent *TM* and *TE* modes, the spectral scattered magnetic components can be got as:

$$\tilde{H}^{sc}_{\varphi n} = -Y^e_c \tilde{E}^{sc}_{\rho n}, \quad \tilde{H}^{sc}_{\rho n} = Y^h_c \tilde{E}^{sc}_{\varphi n} \tag{11}$$

Once the transverse components of scattered fields in spatial domain $E^{sc}_{\rho n}$, $E^{sc}_{\varphi n}$, $H^{sc}_{\rho n}$, $H^{sc}_{\varphi n}$ are solved by means of the inverse vetor Hankel transform of their spectral expressions, the z components E^{sc}_{zn}, H^{sc}_{zn} can also be got according to Maxwell's equations.

NUMERICAL RESULTS

For a FZP with λ/ν phase complement[1],a half-wave $(\nu = 2)$ dual-layer FZP lens with the focal lengths $F_1 = 0.20m$, $F_2 = F_1 - d$, is designed at $f = 9.375GHz$, each layer consists of four (l=*1,2,3,4*) rings. Denote $R = 10\lg\left(|E^{sc}|^2 / |E^{inc}|^2\right)$ is scattered field level in focal region, for single-layer (R_1) or dual-layer (R_2) FZP lens ,the difference ($R_2 - R_1$) is a function of d, which shows the gain enhancement due to the second FZP (Fig.3); and that $d = \lambda/2$ is a best choice, while the field distributions around the focus are shown in Fig.4 and Fig.5, respectively. Obviously, the field intensity is concentrated at focus with a region of 3dB reduction about $2\lambda \times 1.2\lambda$ along and across the focal axis. The results of field distribution are matching the physical characteristics of Fresnel Zone Plate Antenna.

REFERENCES

[1]J.C.Wiltse and J.E.Garret, The Fresnel Zone Plate Antenna, Microwave Journal, Jan., 1991

[2]S.M.Ali, W.C.Chew, Vector Hankel Transform Analysis of Annular-Ring Microstrip Antenna, IEEE, Trans., Vol. AP-30, No.4, July, 1982

[3]W.C.,Chew, T.M.Habashy, the use of Vector Transforms in solving some Electromagnetic Scattering Problems, IEEE Trans., Vol.AP-34, No.7, July., 1986

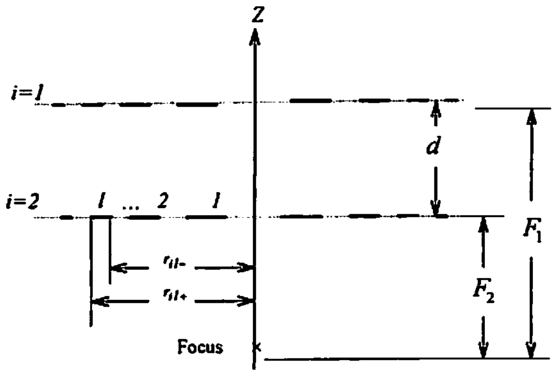

Fig.1 Geometry of dual-layer FZP lens

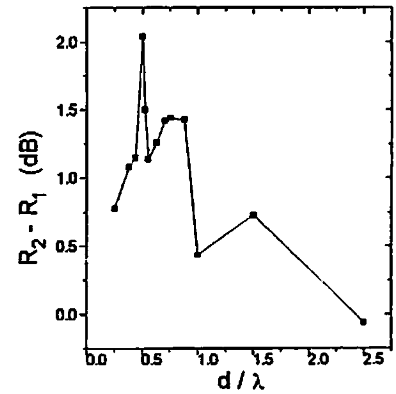

Fig.3. Gain enhancement of the 2nd FZP

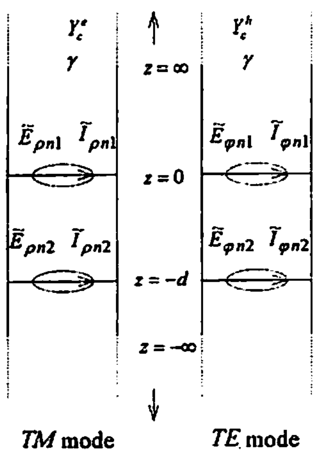

Fig.2 Equivalent circuit of dual-layer FZP lens in spectral domain

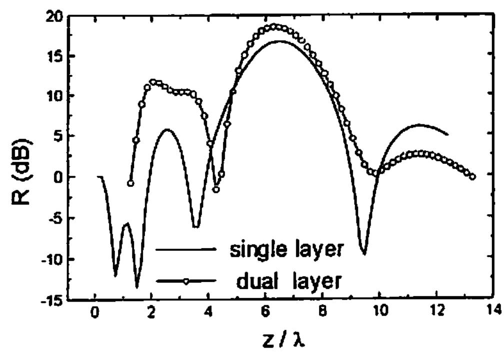

Fig.4 Field intensity along focal axis (d=λ/ 2)

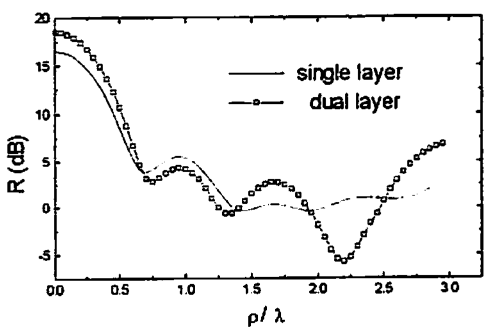

Fig.5 Field intensity across focal axis (d=λ/ 2)